CHEMISTRY
A EUROPEAN JOURNAL

DOI: 10.1002/chem.200601358

QM/MM Modeling of Enantioselective Pybox–Ruthenium- and Box–Copper-Catalyzed Cyclopropanation Reactions: Scope, Performance, and Applications to Ligand Design

José I. García,*[a] Gonzalo Jiménez-Osés,[b] Víctor Martínez-Merino,[c] José A. Mayoral,[a] Elísabet Pires,[a] and Isabel Villalba[a]

In memory of Professor Marcial Moreno-Mañas

Abstract: An extensive comparison of full-QM (B3LYP) and QM/MM (B3LYP:UFF) levels of theory has been made for two enantioselective catalytic systems, namely, Pybox–Ru and Box–Cu complexes, in the cyclopropanation of alkenes (ethylene and styrene) with methyl diazoacetate. The geometries of the key reaction intermediates and transition structures calculated at the QM/MM level are generally in satisfactory agreement with full-QM calculated geometries. More importantly, the relative energies calculated at the QM/MM level are in good agreement with those calculated at the full-QM level in all cases. Furthermore, the QM/MM energies are often in better agreement with the stereoselectivity experimentally observed, and this suggests that QM/MM calculations can be superior to full-QM calculations when subtle differences in inter- and intramolecular interactions are important in determining the selectivity, as is the case in enantioselective catalysis. The predictive value of the model presented is validated by the explanation of the unusual enantioselectivity behavior exhibited by a new bis-oxazoline ligand, the stereogenic centers of which are quaternary carbon atoms.

Keywords: asymmetric catalysis · copper · density functional calculations · N ligands · ruthenium

Introduction

Computational mechanistic studies on transition-metal-catalyzed reactions are valuable tools that can provide useful insights into the mechanisms of these reactions and help in the design of new and more efficient catalytic systems. However, in spite of ever-increasing computing power and better modeling software, computational mechanistic studies on enantioselective catalytic systems continue to be challenging at the quantum-mechanical (QM) level, mainly due to the size of the molecules involved and the large number of reaction channels to be explored. Therefore, in spite of the continually increasing number of thorough full-QM computational studies of enantioselective catalytic systems based on transition-metal complexes, this kind of study is still highly demanding in terms of time and computer resources.

An alternative to QM calculations is the use of specialized force fields, parameterized to include the metal, in molecular mechanics (MM) calculations.[1] However, this approach, although useful for calculating molecular structures, is difficult to apply to the electron reorganization typically occurring in reaction transition structures (TS). Several interesting attempts have been made to parameterize the force field to calculate transition structures of metal-catalyzed reactions, but the method is far from being of general applicability.[2]

Combined QM/MM approaches have found widespread use for treating systems in which only a small part must be

[a] Dr. J. I. García, Dr. J. A. Mayoral, Dr. E. Pires, Dipl.-Chem. I. Villalba
Departamento de Química Orgánica, ICMA
CSIC-Universidad de Zaragoza
Pedro Cerbuna 12, 50009 Zaragoza (Spain)
Fax: (+34) 976-762-077
E-mail: jig@unizar.es

[b] Dipl.-Chem. G. Jiménez-Osés
Departamento de Química
Complejo Científico-Tecnológico
Universidad de La Rioja, 26006 Logroño (Spain)

[c] Dr. V. Martínez-Merino
Departamento de Química Aplicada
Universidad Pública de Navarra
31006 Pamplona (Spain)

Supporting information for this article is available on the WWW under http://www.chemeurj.org/ or from the author.

described with high accuracy by means of a QM treatment. In these cases the remaining part of the system can be considered as an "environment" that exerts steric constraints or acts as a support and can be treated at the MM level. Typical examples of such systems are active sites of enzymes,[3] organic molecule–biomolecule (proteins,[4] nucleic acids[5]) interactions, chemical reactivity in the presence of a solvent,[6] active centers of solid catalysts,[7] large metal complexes or clusters,[8] and homogeneous catalysts with bulky ligands[9] such as those typically found in enantioselective catalysis.[10]

Most implementations of the QM/MM methodology in currently available software are based on a "substractive" approach, such as that used in the IMMOM method[11] and its more general implementation, the ONIOM method.[12]

In terms of modeling catalytic transition-metal complexes, these methods suffer from the drawback that some parameters for the metal and its surrounding atoms must be included in the force field. To overcome this difficulty, the "universal force field" (UFF)[13] is often used, since it includes parameters for most elements in the Periodic Table. However, it is well known that the more general the parameterization of a force field, the less accurate are the results. It is therefore important to determine to what extent using the UFF affords meaningful results when applied to systems for which the difference between an excellent and an unacceptable result is often a matter of a few kilocalories per mole.

Here we present a thorough comparative study of two classes of enantioselective cyclopropanation catalysts (Scheme 1), namely, pyridine bis-oxazoline ruthenium

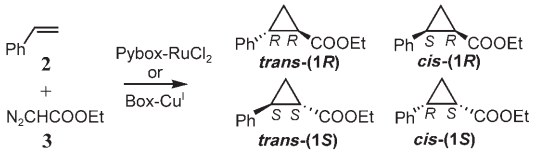

Scheme 1. Model cyclopropanation reaction catalyzed by Pybox-$RuCl_2$ or Box-Cu^I.

(Pybox–Ru) and bis-oxazoline copper (Box–Cu), in which full-QM, QM/MM, and experimental results are compared with the aim of determining the scope of applicability of a standard QM/MM method to modeling these complex systems. Furthermore, the predictive ability of this scheme is tested for the case of a new bis-oxazoline ligand that is structurally different to those usually employed in these reactions.

Results and Discussion

Computational methods: All QM calculations (full-QM and QM part in QM/MM calculations) were carried out by means of the B3LYP hybrid functional[14] because of the satisfactory performance of this technique in the chemistry of transition metals,[15] particularly in the systems studied here.[16,17] Full geometrical optimizations using the LANL2DZ basis set for the Ru complexes and the 6-31G(d) basis set for the Cu complexes were carried out with the Gaussian 03 package.[18] The ONIOM calculations were also carried with the standard implementation in the Gaussian 03 package. The internally stored UFF parameters were used in the MM part of the QM/MM calculations. Analytical frequencies were calculated at the same level used in the geometry optimization, and the nature of the stationary points was determined in each case according to the correct number of negative eigenvalues of the Hessian matrix. Scaled frequencies were not considered in full-QM calculations, since significant errors in the calculated thermodynamic properties are not found at this theoretical level.[19] Unless otherwise stated, only E_0+ZPE energies are used for the discussion of the relative stabilities of the chemical structures considered. Hard data on electronic energies, as well as entropies, enthalpies, Gibbs free energies, and lowest frequencies of the different conformations of all structures considered, are available as Supporting Information.

***i*PrPybox–ruthenium systems**: Recently, we reported a detailed computational mechanistic study on the origin of stereoselectivity in the cyclopropanation of styrene (**2**) with ethyl diazoacetate (**3**) catalyzed by [$RuCl_2$(*i*PrPybox)] (*i*PrPybox: 2,6-bis[(*S*)-4-methyl-4,5-dihydrooxazol-2-yl]pyridine (Scheme 1).[16] This was carried out at a full-QM theoretical level (B3LYP/LANL2DZ) using a molecular model almost identical to the most common experimental system (the only difference was the replacement of the ethyl group of the diazo compound by a methyl group). Therefore, this model system is a good benchmark to test the viability of using QM/MM instead of full-QM calculations. Two-layer ONIOM calculations were envisaged, using the B3LYP/LANL2DZ level for the QM part and the UFF force field for the MM part. The partition scheme of the full systems into their QM and MM parts is shown in Figure 1.

The isopropyl groups of the *i*PrPybox ligand, the methyl group of the ester moiety, and the phenyl group of styrene are treated at the MM level, whereas the rest of the system is kept at the QM level. Preliminary studies showed that the oxazoline rings must be kept in the QM part in order to obtain reasonable geometries. The treatment of the phenyl group of styrene at the MM level warrants a more detailed explanation. Of course, this choice results in the loss of con-

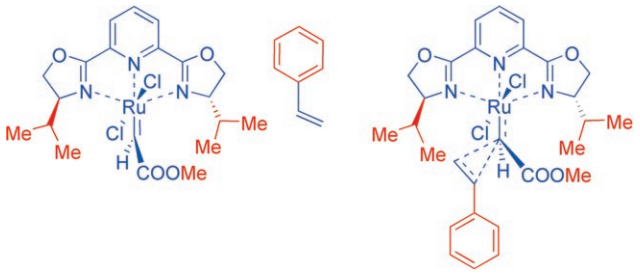

Figure 1. QM/MM partition scheme used in the calculations. Blue: QM part, red: MM part.

jugation between the reacting double bond and the phenyl group, which, in turn, will result in changes in the synchronicity and the energy of the transition states.

It has been shown by some authors that keeping a butadiene structure in the QM part is effective in preserving this important electronic feature of the system.[20] However, we were particularly interested in testing the reliability of the chosen partition scheme because of its implications in the case of the Box–Cu catalysts (see below).[21]

The calculated activation barriers and relative energies of the corresponding transition structures (TS), calculated both at the B3LYP/LANL2DZ[16] and the ONIOM(B3LYP/LANL2DZ:UFF) levels, are given in Table 1. Here **c** and **t** stand for the relative position of the styrene phenyl and the carbene ester groups, leading to the corresponding *cis* and *trans* cyclopropanes, respectively; **Re** and **Si** stand for the stereoface of the carbene carbon atom to which the alkene approaches, which determines the absolute configuration of C^1 of the cyclopropane products (for this reaction, *Re* approach leads to (1*R*)-cyclopropanes, and *Si* approach to (1*S*)-cyclopropanes). Finally, **I** and **II** stand for the conformation of the carbene ester group. In the **I** conformation, the carbonyl oxygen atom is far from the approaching alkene, whereas in the **II** conformation it points towards to the alkene. A graphical representation of these geometric relationships is depicted in Figure S2 in the Supporting Information.

Table 1. Calculated activation barriers and relative energies [kcal mol^{-1}] of the corresponding transition structures (TS)[a] at the B3LYP/LANL2DZ (full-QM) and ONIOM(B3LYP/LANL2DZ:UFF) (QM/MM) levels and calculated *ee* [%].

	Full-QM[16]					QM/MM				
TS	$\Delta E^{\neq}$	$\Delta\Delta E^{\neq}$	$\Delta G^{\neq}$	$\Delta\Delta G^{\neq}$	*ee*	$\Delta E^{\neq}$	$\Delta\Delta E^{\neq}$	$\Delta G^{\neq}$	$\Delta\Delta G^{\neq}$	*ee*
5tReI	8.2	**0.0**	24.6	0.1	95	12.0	**0.0**	28.2	**0.0**	94
5tReII	8.7	0.5	24.5	**0.0**		12.0	**0.0**	28.2	**0.0**	
5tSiI	10.9	2.7	26.3	1.8		14.1	2.1	29.9	1.7	
5tSiII	11.9	3.7	28.2	3.7		16.2	4.2	31.9	3.7	
5cReI	11.6	3.4	27.2	2.7	77	12.8	**0.8**	28.9	**0.7**	97
5cReII	11.0	**2.8**	27.0	**2.5**		13.6	1.6	29.3	1.1	
5cSiI[b]	13.2	5.0	27.9	3.4		15.5	3.5	31.2	3.0	
5cSiII	14.7	6.5	30.6	6.1		16.8	4.8	32.8	4.6	

[a] **t** and **c** stand for *trans* and *cis* approaches of styrene to the carbene ester group, **Re** and **Si** for the face of the carbene carbon atom approached by styrene, and **I** and **II** for the conformation of the ester group (**I**: carbonyl oxygen far from the approaching alkene, **II**: carbonyl oxygen near to the approaching alkene). [b] This work.

As expected, the calculated activation barriers are higher at the ONIOM level due to the lack of conjugation with the phenyl group. Indeed, they are closer (but systematically lower, that is, steric effects can also play a role in activation barriers) to the barriers calculated for the reaction with ethylene (**1**) at the B3LYP/LANL2DZ level (calculated lowest activation barriers: 15.3 kcal mol^{-1} for *Re* approach and 19.3 kcal mol^{-1} for *Si* approach; calculated Gibbs free activation energies: 30.4 kcal mol^{-1} for *Re* approach and 34.3 kcal mol^{-1} for *Si* approach). However, and more importantly, the relative energies of the different TS **5**, which determine the stereoselectivity of the reaction under Curtin–Hammett conditions, are very similar for the *trans* TS (**5t**) when considering either electronic or Gibbs free energies at both theoretical levels. In the case of the *cis* TS (**5c**), the relative energies tend to be somewhat lower in the QM/MM calculations (with an average difference of ca. 2 kcal mol^{-1} with respect to the full-QM values) but, interestingly, this leads to a better agreement with the experimental *trans*/*cis* stereoselectivity. Thus, the QM/MM results allow an estimation of the *trans/cis* selectivity (based on the Boltzmann distribution obtained from Gibbs free energies) of 81:19, whereas the experimental value for the same system is 89:11.[22] On the other hand, the full-QM calculations predict an almost total *trans* selectivity (>99:1). This result can be explained by the deficient treatment of dispersion forces at the DFT level of theory,[23] which probably results in overestimation of the steric repulsions between the phenyl and the ester groups in the *cis* TS.

Concerning enantioselectivities, the QM/MM calculations are in complete agreement with the absolute configurations of the major cyclopropanes experimentally observed, that is, preferential approach of styrene to the *Re* face of the carbene carbon atom leads to (1*R*)-cyclopropanes. From a quantitative point of view, the QM/MM values are also very close to the full-QM ones, so that high enantioselectivities are predicted for both *trans*- and *cis*-cyclopropanes. However, as before, the QM/MM values lead to values that are slightly closer to those obtained experimentally for the same system (94 vs. 92% *ee*[17] for *trans*-cyclopropanes and 97 vs. 97% *ee*[17] for *cis*-cyclopropanes).

It is interesting to put these energy values in the context of the calculated geometries. Table 2 lists the calculated C–C bond-forming distances in the corresponding TS (C_α–$C_{carbene}$ and C_β–$C_{carbene}$), together with the C_β-$C_{carbene}$-Cu-N torsion angle, which has been shown to be indicative of the steric interactions present in the different TS.[16] As can be seen, the QM/MM calculations reproduce well the larger torsion angles observed in the *Si* TS (values in boldface in the Table), which in turn result in higher energies for stereoelectronic reasons.[16] A general view of the main geometric differences observed between full-QM and QM/MM calculations can be seen by superposing each pair of analogous structures. The RMS-minimized overlay of **5tReI**, **5tSiI**, **5cReII**, and **5cSiII** (those of minimum energy leading to each of the four possible cyclopropane products in the full-QM calculations) is shown in Figure 2.

The main geometrical differences lie in the position of the phenyl group, which can be explained by the lack of conju-

Table 2. Calculated C_α–$C_{carbene}$ (d_1) and C_β–$C_{carbene}$ (d_2) bond-forming distances [Å] and C_β–$C_{carbene}$-Ru-N torsion angles Φ [°] in the transition structures[a] at the B3LYP/LANL2DZ (full-QM) and the ONIOM (B3LYP/LANL2DZ:UFF) (QM/MM) levels.

	Full-QM[16]				QM/MM			
TS	d_1	d_2	Δd	Φ	d_1	d_2	Δd	Φ
5tReI	2.106	2.718	0.612	21	2.029	2.493	0.464	24
5tReII	2.122	2.719	0.597	31	2.070	2.481	0.411	40
5tSiI	2.127	2.711	0.584	**60**	2.030	2.509	0.479	**69**
5tSiII	2.102	2.715	0.613	**43**	2.003	2.515	0.512	**54**
5cReI	2.075	2.705	0.630	22	1.993	2.475	0.482	24
5c-ReII	2.105	2.724	0.619	31	2.021	2.462	0.441	30
5cSiI[b]	2.102	2.736	0.634	**61**	1.995	2.476	0.481	**60**
5cSiII	2.068	2.717	0.649	**46**	1.967	2.496	0.529	**50**

[a] **t** stands for *trans* approach of styrene to the carbene ester group, **Re** and **Si** for the face of the carbene carbon atom approached by styrene, and **I** and **II** stand for the conformation of the ester group (**I**: carbonyl oxygen far from the approaching alkene, **II**: carbonyl oxygen near to the approaching alkene). [b] This work.

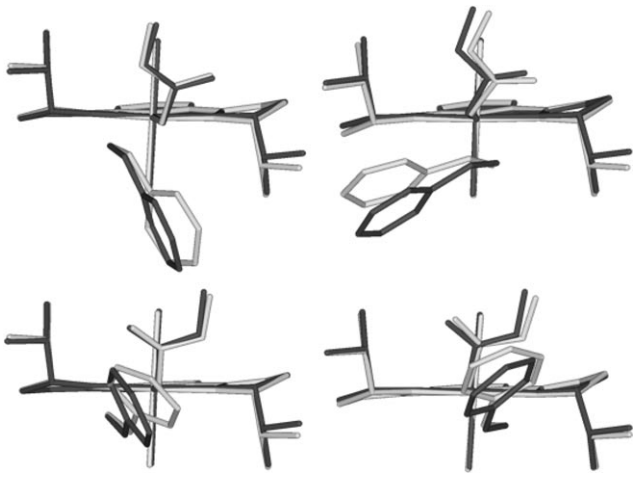

Figure 2. Overlay of **5tReI**, **5tSiI**, **5cReII**, and **5cSiII** TS, calculated at the full-QM B3LYP/LANL2DZ (dark gray) and QM/MM ONIOM (B3LYP/LANL2DZ:UFF) (light gray) levels of theory.

gation and the different treatment of the dispersion forces, as explained above. The rest of the structure looks very similar in all cases and, based on energy and geometry results, we can therefore conclude that QM/MM calculations are adequate in this system to gain insights into the stereodifferentiation mechanisms. Indeed, this approach is also acceptable for estimating the stereoselectivities expected, at least in a semiquantitative manner, in spite of the significant simplification introduced by considering the phenyl group in the MM part of the model.

***t*BuBox–copper systems**: Several computational mechanistic studies on the mechanism of copper-catalyzed cyclopropanation reactions have recently been published.[17,24–27] In particular, the enantiodifferentiation mechanism in the case of bis-oxazoline–Cu catalysts has been studied by us[17] and by Norrby and co-workers,[24] who used a QM/MM scheme to model the chiral ligand.

A recurrent problem in these theoretical studies is that the prototypical cyclopropanation reaction, that is, the cyclopropanation of styrene with alkyl diazoacetates, cannot be explicitly investigated because of the lack of convergence in the transition-structure searches. This problem is probably due to the inadequacy of B3LYP to describe the potential-energy surface (PES) in the neighborhood of the TS, which leads to a monotonously downhill PES in the case of substituted alkenes such as styrene. Norrby et al. estimated a barrier in the Gibbs free energy surface of about 1 kcal mol using a composed method. This fact is undoubtedly due to the extra stabilization of the TS by delocalization of the incipient positive charge developed at the α-carbon atom of styrene in the highly asynchronous TS. In fact, convergence problems in TS searches are found even when the reacting double bond is substituted with a single methyl group (propene);[17a] hence, *cis*/*trans* diastereoselectivity becomes difficult to investigate and, furthermore, structural models close to the experimental systems usually studied cannot be treated at a full-QM level.

In our previous studies on the enantioselective cyclopropanation reaction involving chiral cationic bis-oxazoline Cu complexes, we used ethylene (**1**) as alkene and bis[4-(*S*)-methyl-4,5-dihydrooxazol-2-yl]methane, a bis-oxazoline bearing methyl groups on the stereogenic centers, as chiral ligand. Although this simplification proved to be useful to gain insights into the mechanism of enantiodifferentiation, the real ligands bear much bulkier groups (e.g., *tert*-butyl, phenyl, or indanyl groups). We therefore decided to start by performing full-QM [B3LYP/6-31G(d)] calculations on the main stationary points in the reaction profile of the cyclopropanation of ethylene (**1**) with methyl diazoacetate (**3**), catalyzed by the Cu^I complex of 2,2-bis[4-(*S*)-*tert*-butyl-4,5-dihydrooxazol-2-yl)propane] (*t*BuBox–Cu), that is, the same complex used in many previous experiments. The corresponding catalytic cycle is shown in Scheme 2. The results obtained were then compared with those of the QM/MM calculations using the partition scheme shown in Figure 3.

The calculated activation barriers and relative energies of the corresponding intermediates and transition structures, calculated both at the B3LYP/6-31G(d) and the ONIOM(B3LYP/6-31G(d):UFF) levels, are listed in Table 3. The main geometrical features of the key intermediates and transition structures on the reaction profile are shown in Figure 4. Complex **6** is the precatalytic *t*BuBox-Cu ethylene complex, which evolves into a *t*BuBox-Cu methyl diazoacetate complex (not shown) by an associative ligand-exchange mechanism.[17] Complex **7** is the nitrogen extrusion TS, corresponding to the rate-determining step, **8** is the key *t*BuBox-Cu carbene intermediate, and **9** is the alkene addition TS. Although the model complexes are positively charged, we have previously shown[17] that solvent effects do not

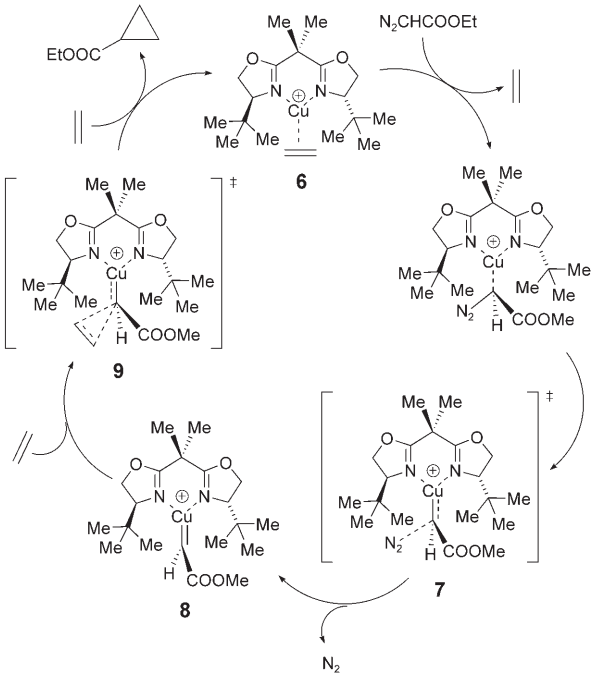

Scheme 2. Catalytic cycle for the cyclopropanation of ethylene (**1**) with methyl diazoacetate (**3**) catalyzed by the *t*BuBox–Cu complex.

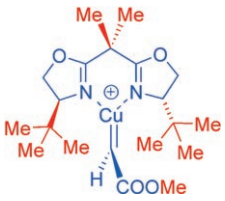

Figure 3. QM/MM partition scheme used in the calculations with *t*BuBox. Blue: QM part, red: MM part.

Table 3. Calculated activation barriers and relative energies[a] [kcal mol^{-1}] of the corresponding intermediates and transition structures (TS)[b] at the B3LYP/6-31G(d) (full-QM) and the ONIOM(B3LYP/6-31G(d):UFF) (QM/MM) levels.[c]

Structure	Full-QM		QM/MM	
	ΔE	$\Delta\Delta E^{\neq}$	ΔE	$\Delta\Delta E^{\neq}$
6	0.0	–	0.0	–
7	20.0	–	20.6	–
8	3.7	–	2.6	–
9ReI	1.2	**0.0**	4.5	**0.0**
9ReII	3.2	2.0	6.1	1.6
9SiI	3.1	1.9	6.0	1.5
9SiII	2.9	1.7	5.8	1.3

[a] Energies include zero-point energy (ZPE) corrections at the same level of theory. [b] **t** and **c** stand for *trans* and *cis* approaches of styrene to the carbene ester group, **Re** and **Si** for the face of the carbene carbon approached by styrene, and **I** and **II** for the conformation of the ester group (**I**: carbonyl oxygen far from the approaching alkene, **II**: carbonyl oxygen near to the approaching alkene). [c] The initial *t*BuBox–Cu ethylene complex (**6**), ethylene (**1**), methyl diazoacetate, and dinitrogen were arbitrarily chosen as the zero level in the relative-energy calculations. **7** is the nitrogen extrusion TS and **8** the Cu carbene intermediate.

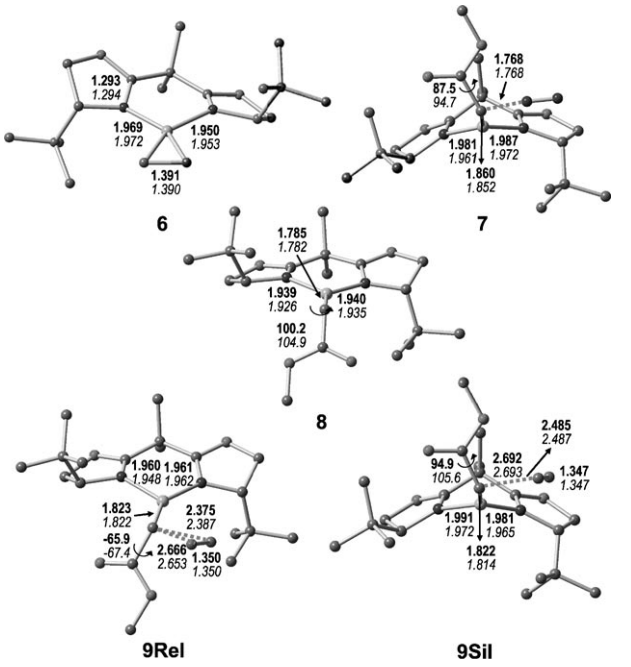

Figure 4. Some selected geometrical parameters of the main intermediates and transition structures of the reaction of ethylene with methyl diazoacetate catalyzed by *t*BuBox–Cu complex, calculated at the B3LYP/6–31G(d) (boldface) and ONIOM (B3LYP/6-31G(d):UFF) (normal face) levels of theory.

have significant influence on the relative energies of the carbene insertion TS. On the other hand, others have reported[24] that the solvation contribution changes substantially along the reaction coordinate. Continuum dielectric solvation models cannot be used together with ONIOM calculations in the current version of Gaussian software, but an estimation of the differential solvation of the different TS can be obtained by means of single-point energy calculations at the full-QM level. We carried out such calculations for **9ReI** and **9ReII**, and found that the difference in solvation energy is less than 0.5 kcal mol^{-1}, in agreement with our previous results, so that gas-phase results can be confidently used to assess stereodifferentiation in these systems.

As can be seen from the results in Table 3, both the activation barriers and the relative energies of the four possible TS for carbene insertion (**9**) into the ethylene double bond show excellent agreement when full-QM and QM/MM results are compared. As a consequence, QM/MM calculations can be confidently used in these systems to explore the possible reaction paths and, more interestingly, to develop enantiodifferentiation models for new, related catalytic systems. In this regard, it is noteworthy that the relative energies of the four insertion TS follow the same trend in the full-QM and QM/MM calculations.

From a geometrical point of view, QM/MM results also display remarkable agreement with full-QM calculated geometries, as can be seen in the general views and principal geometric parameters shown in Figure 4. The calculated structures for the four possible TS allow us to conclude that

the main steric reason for the preferential approach of ethylene to the *Re* face of the carbene carbon atom lies in the interaction between the ester group of the carbene moiety and the *tert*-butyl group of the chiral ligand in the *Si* approach, as previously established with simpler models.[17] The TS are earlier for *Si* approach of ethylene, a fact that is also well reproduced by the QM/MM calculations. The important steric hindrance of the *tert*-butyl group in the *Si* approach results in a remarkable deformation of the six-membered copper chelate, which gives rise to a boat conformation in which the *tert*-butyl and ester groups are better accommodated. A similar geometric deformation is observed in dinitrogen extrusion TS **7**.

To gain insights into enantio- and diastereoselectivity, QM/MM calculations were carried out with the same partition scheme as described for styrene (**2**) in the preceding section. This approach was taken due to the aforementioned difficulties in carrying out a full-QM theoretical study. The main energy results for the reaction pathway of the catalytic cycle are given in Table 4.

Table 4. Calculated activation barriers and relative energies[a] [kcal mol^{-1}] of the corresponding intermediates and transition structures (TS)[b] at the ONIOM(B3LYP/6-31G(d):UFF) level.[c]

Structure	ΔE	$\Delta\Delta E^{+}$
10[c]	0.0	–
7	26.8	–
8	8.8[d]	–
11tReI	8.1	**0.0**
11tReII	10.3	2.2
11tSiI	9.8	1.7
11tSiII	9.5	1.4
11cReI	8.4	**0.4**
11cReII	11.1	3.0
11cSiI	10.1	2.0
11cSiII	9.9	1.8

[a] Energies include zero-point energy (ZPE) corrections at the same level of theory. [b] **t** and **c** stand for *trans* and *cis* approaches of styrene to the carbene ester group, **Re** and **Si** for the face of the carbene carbon atom approached by styrene, and **I** and **II** for the conformation of the ester group (**I**: carbonyl oxygen far from the approaching alkene, **II**: carbonyl oxygen near to the approaching alkene). [c] The initial *t*BuBox–Cu styrene complex, styrene, methyl diazoacetate, and dinitrogen were arbitrarily chosen as the zero level in the relative-energy calculations. [c] *t*BuBox–Cu styrene complex. [d] Relative to the *t*BuBox–Cu styrene complex **10**.

The calculated energy profile is very similar to that previously calculated for the ethylene model, as one would expect given that the phenyl group of styrene is considered only in the MM part. The calculated *cis*/*trans* diastereoselectivity and the enantioselectivities in *trans* and *cis* cyclopropane products are in good agreement with experimental observations. Thus, the calculated *trans*/*cis* selectivity is about 65/35 (experimental 73/27).[28] The calculated enantioselectivies are about 75% both for *trans* and *cis* cyclopropanes, whereas the experimental *ee* values are greater than 95%.[28] The use of E_0 energy values instead of E_0+ZPE gives better agreement with experimental results (ca. 95% *ee* for both *trans* and *cis* products). Note, however, that this model is not intended to provide quantitative agreement with experiments (because of the evident simplifications), but only to show the general trends of the reaction mechanism and to gain insights into the origin of the stereodifferentiation. In our opinion, the results described in Table 4 are good enough for these purposes.

The geometries of the lowest energy TS leading to the four possible cyclopropane products (**11tReI**, **11tSiI**, **11cReII**, and **11cSiII**) are shown in Figure 5.

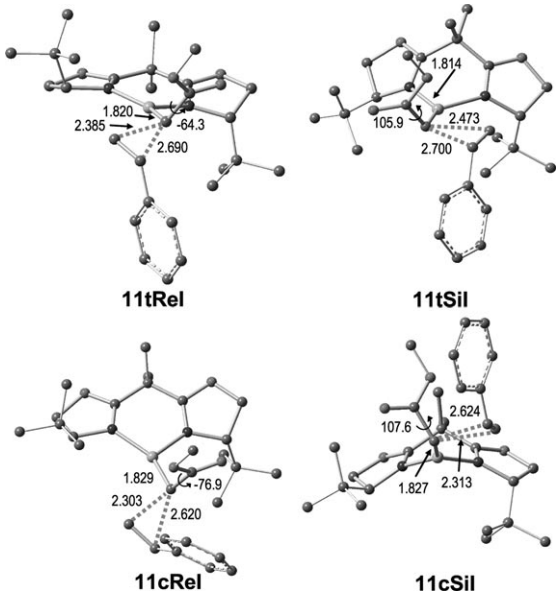

Figure 5. Some selected geometrical parameters of the lowest energy transition structures in the reaction of styrene with methyl diazoacetate catalyzed by *t*BuBox–Cu complex, calculated at the ONIOM(B3LYP/6-31G(d):UFF) level of theory.

As expected, the main geometrical parameters are very similar to those previously described for the ethylene model. However, some significant differences between the four TS can be noted. For example, *trans* TS are earlier than *cis* TS (both C–C bond-forming distances are longer). Furthermore, the synchronicities of the four TS are also different, with Δd ranging from 0.227 to 0.317 Å. These results show that the steric effect introduced by the phenyl group, even if only considered in the MM part, is able to lead to significant changes in the position of the TS on the reaction coordinate.

PhBox–copper systems: To further test the reliability of this methodology we calculated a system that has not been considered in previous theoretical studies, despite the fact that it is one of the most widely used in catalytic applications, namely, the 2,2-bis[4-(*S*)-phenyl-4,5-dihydrooxazol-2-yl)propane] Cu complex (PhBox–Cu). The partition scheme used to assign the QM and MM layers is shown in Figure 6. In this partition both phenyl groups are kept in the MM part since their effect on the stereoselectivity of the reactions is presumably due to steric effects. In this way the QM layer is

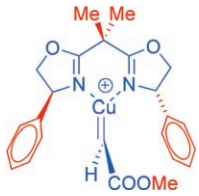

Figure 6. QM/MM partition scheme used in the calculations with PhBox. Blue: QM part, red: MM part.

the same as that previously considered in the *t*BuBox calculations.

By following the same protocol as used in the previous calculations, we first compared full-QM and QM/MM calculations for the reaction of ethylene (**1**) with methyl diazoacetate (**3**) catalyzed by the PhBox-Cu complex, in order to detect any possible significant difference between the two theoretical levels. These calculations again showed excellent agreement in terms of relative energies and geometries of the carbene insertion TS (**15**). The RMS-minimized overlay of the TS calculated at the two theoretical levels is shown in Figure 7.

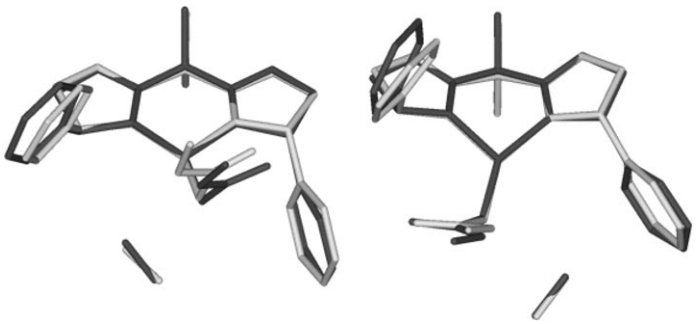

Figure 7. Overlay of the **15ReI** and **15SiI** TS, calculated at the full-QM B3LYP/6-31G(d) (dark gray) and QM/MM ONIOM (B3LYP/6-31G(d):UFF) (light gray) levels of theory.

We next calculated the reaction pathway for the cyclopropanation of styrene (**2**) with methyl diazoacetate (**3**) catalyzed by the PhBox-Cu complex. The main energy results are listed in Table 5.

The most remarkable difference in comparison with the previously described systems is the existence of several transition structures for the approach of styrene to the *Si* face of the carbene in the *trans* position (TS **17tSi**). For this reaction trajectory, up to four transition structures could be located and properly characterized, and in these, apart from the conformation of the ester group, variations in the bending of the chelate complex and in the conformation of one of the phenyl groups of the ligand could be detected. Otherwise, the existence of multiple transition structures for this reaction channel does not have significant consequences for the stereoselectivity of the reaction, as can be seen by examining the energy values in Table 5. The geometries of the lowest energy TS leading to the four possible cyclopropane products (the two different geometries shown for **17tSi** display different chelate conformations) are shown in Figure 8. All of the calculated structures can be found in the Supporting Information.

Table 5. Calculated activation barriers and relative energies[a] [kcal mol^{-1}] of the corresponding intermediates and transition structures (TS)[b] at the ONIOM(B3LYP/6-31G(d):UFF) and B3LYP/6–31G(d)//ONIOM-(B3LYP/6-31G(d):UFF) levels.[c]

TS	ΔE_{ONIOM}	$\Delta\Delta E^{\neq}_{ONIOM}$	$\Delta\Delta E^{\neq}_{SP}$
16[d]	0.0		
13	31.8		
14	15.6[e]		
17tReI	10.2	**0.0**	**0.0**
17tReII	12.1	1.9	1.8
17tSiI	14.8	4.6	2.8
17tSiII	14.7	4.5	9.1
17tSiIII	15.3	5.1	2.6
17tSiIV	15.5	5.3	3.3
17cReI	11.7	**1.5**	1.9
17cReII	13.6	3.4	4.5
17cSiI	15.1	4.9	1.8
17cSiII	15.0	4.8	**1.1**

[a] Energies include zero-point energy (ZPE) corrections at the same level of theory. [b] **t** and **c** stand for *trans* and *cis* approaches of styrene to the carbene ester group, **Re** and **Si** for the face of the carbene carbon atom approached by styrene, and **I** and **II** for the conformation of the ester group (**I**: carbonyl oxygen far from the approaching alkene, **II**: carbonyl oxygen near to the approaching alkene). [c] The initial PhBox–Cu styrene complex, styrene, methyl diazoacetate, and dinitrogen were arbitrarily chosen as the zero level in the relative-energy calculations. [d] PhBox–Cu styrene complex. [e] Relative to PhBox–Cu styrene complex **16**.

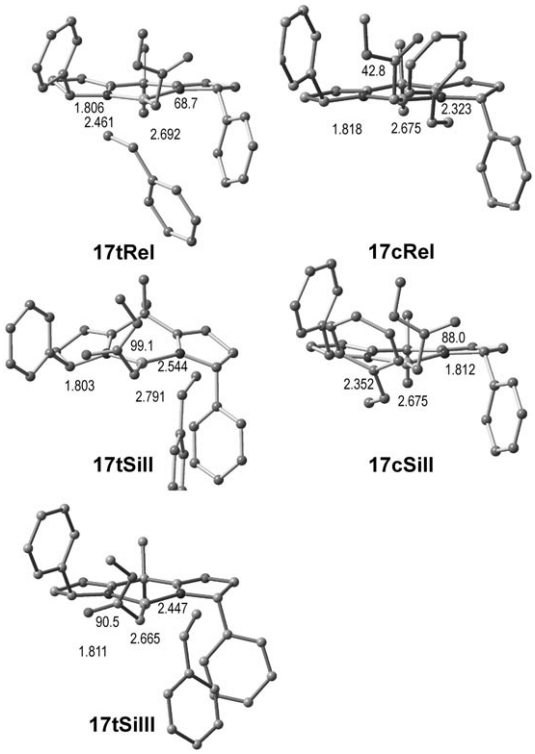

Figure 8. Some selected geometrical parameters of the lowest energy transition structures of the reaction of styrene with methyl diazoacetate catalyzed by PhBox–Cu complex, calculated at the ONIOM(B3LYP/6-31G(d):UFF) level of theory.

As in the previously studied systems, the calculated stereoselectivities are in agreement with the experimental results observed for the analogous systems, at least in a qualitative manner. Thus, the formation of *trans*-cyclopropanes is favored over that of *cis*-cyclopropanes, even though the calculated *trans*:*cis* selectivity is overestimated (ca. 90:10 vs. experimental 70:30). The enantioselectivities are also overestimated (>95% *ee* for both pairs of cyclopropane diastereomers, whereas the experimental values are closer to 50–60% *ee*).[29] The question arises whether these numerical values could be improved by carrying out full-QM single-point energy calculations on the QM/MM calculated geometries. To evaluate this possibility, B3LYP/6-31G(d)//ONIOM(B3LYP/6-31G(d):UFF) single-point energy calculations were performed on all stationary points calculated for the reaction pathway. The main results are gathered in Table 5 (ΔE_{SP} values). Although the calculated *trans*:*cis* selectivity (ca. 75:25) is closer to the experimental value, the enantioselectivity for *trans*-cyclopropanes is still too high (>95% *ee*) and, more importantly, the major *cis*-cyclopropane is predicted to have the opposite configuration to that experimentally observed, with a calculated enantioselectivity of about 70% *ee*. We can therefore conclude, as in the case of the Pybox–Ru systems, that the QM/MM results are superior to the full-QM ones (at least in the single-point energy calculations) when compared with the experimental values and therefore that QM/MM calculations with the partition schemes presented here are valuable tools to model this kind of diastereo- and enantioselective catalytic system.

Some attention must be paid to the differences in computing time when full-QM and QM/MM calculations are compared. As summarized in Table 6, a dramatic reduction of CPU time occurred when computing direct SCF frequencies (the most time-consuming part of the calculations) on changing from full-QM to QM/MM methods in frequency calculations.

Table 6. Full-QM (boldface) versus QM/MM (normal face) computational requirements. Average CPU times [min] were estimated from frequency calculations performed for each set of TS.

TS	Atoms	Basis sets	Primitive Gaussians	Average CPU time [min]	CPU time saving [%]
5	73/38	423/270	1089/692	2278/356	84
9	67/29	532/323	1040/644	2390/287	88
15	63/29	576/323	1120/644	2320/264	89

Optimization times are more difficult to compare, since the number of optimization cycles strongly depends on the starting geometry, which was generally different for full-QM and QM/MM calculations. However, estimations from the CPU time per optimization cycle in different calculations indicate that time savings of between 85 and 95%, in the most favorable case, can be obtained in the QM/MM calculations.

Application to ligand design: The ultimate test for any molecular model is to predict the behavior of a totally new system that has not previously been investigated experimentally, so that the methodology can be used for the rational design of new chiral ligands. Recently, we described[30] the synthesis of a new chiral bis-oxazoline ligand derived from (*S*)-2-methylphenylglycinol, that is, 2,2-bis[(*S*)-4-methyl-4-phenyl-4,5-dihydrooxazol-2-yl)propane] (MePhBox), in which the stereogenic centers in the resulting bis-oxazoline are quaternary carbon atoms. This kind of chiral ligand allows the assessment of the "additivity" of steric effects in the enantioselectivity. The aforementioned ligand can thus be considered to be the result of merging the two simpler bis-oxazoline ligands bearing only either phenyl or methyl groups in the stereogenic centers (Figure 9).

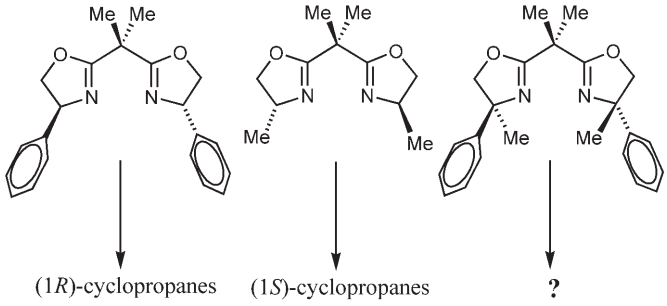

Figure 9. New chiral ligand MePheBox and the "parent" ligands PhBox and MeBox.

It is clear that methyl and phenyl groups must direct toward opposite major enantiomer of the *trans*- and *cis*-cyclopropane products, whereby the absolute configuration of the major products is determined by the best enantiodiscriminant group. As discussed previously, PhBox leads to 60% *ee* in *trans*-cyclopropanes and to 55% *ee* in *cis*-cyclopropanes in the cyclopropanation of styrene with ethyl diazoacetate,[29a] with (1*R*)-cyclopropanes being the major products when the oxazoline has the *S* configuration of the stereogenic centers. This allows a $\Delta\Delta G^{\neq}$ value of 0.7–0.8 kcal mol^{-1} between the TS leading to each cyclopropane enantiomer to be estimated. To the best of our knowledge, experimental results have not yet been reported for the use of MeBox as the chiral ligand. The most similar ligand would be *i*PrBox, for which an enantioselectivity of 40–45% *ee* has been described for the same reaction (hence a $\Delta\Delta G^{\neq}$ value of 0.5–0.7 kcal mol^{-1} between the TS leading to each cyclopropane enantiomer).[28] Assuming similar behavior for the MeBox system, it would be expected that (1*R*)-cyclopropanes would be the major products obtained with MePhBox and that there would be a low enantioselectivity (ca. 15% *ee*, corresponding to $\Delta\Delta G^{\neq} \approx 0.2$ kcal mol^{-1}), given the opposite effect of phenyl and methyl groups. In an effort to test this hypothesis we conducted the experimental and theoretical studies in parallel and obtained surprising but coherent results.

The cyclopropanation of styrene with ethyl diazoacetate catalyzed by MePhBox-Cu (corresponding to TS **18**) led to the (1*S*)-cyclopropanes as major products, with 15% *ee* in

the *trans*-cyclopropanes and 30% *ee* in the *cis*-cyclopropanes, which correspond to $\Delta\Delta G^{\neq}$ values of 0.2 and 0.4 kcal mol^{-1}, respectively. This situation is in contrast to that intuitively expected. On the other hand, the QM/MM theoretical calculations on this system correctly predicted the absolute configuration of the major products (Table 7), albeit with an overestimation of the enantioselectivity (36% *ee* in the *trans*-cyclopropanes and 99% *ee* in the *cis*-cyclopropanes, based on calculated Gibbs free energies).

Table 7. Calculated (ONIOM(B3LYP/6–31G(d):UFF level) relative energies[a] [kcal mol^{-1}] of the transition structures of the cyclopropanation reactions with the PhMeBox and MeBox ligands.

TS	$\Delta\Delta E_{ONIOM}$	Calcd *ee* [%][b]	Exptl *ee* [%]	TS	$\Delta\Delta E_{ONIOM}$	Calcd *ee* [%][b]	Exptl *ee* [%]
18tReI	1.1			**19tReI**	1.5		
18tReII	1.6			**19tReII**	3.2		
18tSiI	2.0	36	20	**19tSiI**	**0.0**	98	66
18tSiII	2.6			**19tSiII**	2.1		
18tSiIII	**0.1**						
18cReI	2.1			**19cReI**	2.1		
18cReII	3.9			**19cReII**	2.9		
18cSiI	**0.0**	99	40	**19cSiI**	**0.1**	94	62
18cSiII	2.0			**19cSiII**	2.5		
18cSiIII	0.4			–	–		
18cSiIV	1.0			–	–		

[a] Energies include zero-point energy (ZPE) corrections at the same level of theory. [b] Based on calculated Gibbs free energies at the same level of theory.

This result seems to point to the methyl group being more stereodirecting than expected, a situation that was experimentally demonstrated when the same cyclopropanation reaction was carried out with the MeBox ligand (corresponding to TS **19**). Surprisingly, the experimental enantioselectivities obtained in *trans*- (66% *ee*) and *cis*-cyclopropanes (62% *ee*) were slightly higher than those obtained with PhBox and much higher than those reported for *i*PrBox. The QM/MM calculations were also in qualitative agreement with these observations (Table 7, calculated enantioselectivities are 98% *ee* in the *trans*-cyclopropanes and 94% *ee* in the *cis*-cyclopropanes, based on calculated Gibbs free energies), and this again demonstrates the usefulness of these kinds of calculations for modeling these enantioselective catalytic systems and even for successfully predicting the behavior of new ligands in these reactions.

Conclusion

An extensive comparison of full-QM (B3LYP) and QM/MM (B3LYP:UFF) levels of theory has been performed for two enantioselective catalytic systems, namely, Pybox–Ru and Box–Cu complexes in the cyclopropanation of alkenes (ethylene and styrene) with methyl diazoacetate. The geometries of the key reaction intermediates and transition structures calculated at the QM/MM level are generally in satisfactory agreement with full-QM calculated geometries. More importantly, the relative energies calculated at the QM/MM level are in good agreement with those calculated at the full-QM level in all cases. Furthermore, the QM/MM energies are often in better agreement with the stereoselectivities experimentally observed, and this suggests that QM/MM calculations can be superior to full-QM calculations when subtle differences in inter- and intramolecular interactions are important in determining the selectivity, as is the case in enantioselective catalysis. The QM/MM calculations were carried out with standard theoretical methods and widely available software, and represent a significant time saving over full-QM approaches on similar systems. These findings open the door to a more general and reliable application of this methodology for other complex systems. The predictive value of the model presented is validated by the explanation of the unusual enantioselectivity exhibited by a new bis-oxazoline ligand, the stereogenic centers of which are quaternary carbon atoms.

Experimental Section

The 2,2-bis[(*S*)-4-methyl-4-phenyl-4,5-dihydrooxazol-2-yl)propane] and 2,2-bis[(*S*)-4-methyl-4.5-dihydrooxazol-2-yl)propane] ligands were prepared as previously described.[30] The bis-oxazoline copper complexes were prepared by dissolving the copper salt ($Cu(OTf)_2$, 0.05 mmol) and the ligand (**19** or **20**, 0.05 mmol) in anhydrous dichloromethane (1 mL). After the mixture had been stirred for 1 h, the insoluble materials were removed by microfiltration and the bluish green solution was added to a mixture of styrene (520.75 mg, 5 mmol), *n*-decane (100 mg), and anhydrous CH_2Cl_2 (4 mL) under an Ar atmosphere. Ethyl diazoacetate (570.5 mg. 5 mmol) in anhydrous CH_2Cl_2 (1 mL) was slowly added (4 h) using a syringe pump. The reaction mixture was stirred at room temperature for 24 h. After this time the solution was diluted with CH_2Cl_2 (5 mL) and the results of the reaction were determined by gas chromatography (FID from Hewlett-Packard 5890II; cross-linked methyl silicone column: 25 m × 0.2 mm × 0.33 μm; helium as carrier gas. 20 psi; injector temperature: 230 °C; detector temperature: 250 °C; oven temperature program: 70 °C (3 min), 15 °C min^{-1} to 200 °C (5 min); retention times: ethyl diazoacetate 4.28 min, styrene 5.03 min. *n*-decane 6.93 min. *cis*-cyclopropanes 11.84 min, *trans*-cyclopropanes 12.35 min). The asymmetric inductions of the reactions were also determined by gas chromatography (FID from Hewlett-Packard 5890II; Cyclodex B column: 30 m × 0.25 mm × 0.25 μm; helium as carrier gas. 20 psi; injector temperature: 230 °C; detector temperature: 250 °C; oven temperature program: 125 °C isothermal; retention times: (1*S*,2*R*)-cyclopropane 28.9 min, (1*R*,2*S*)-cyclopropane 29.8 min, (1*R*,2*R*)-cyclopropane 34.3 min, (1*S*,2*S*)-cyclopropane 34.9 min.

Acknowledgements

This work was made possible by the financial support of the Gobierno de Navarra (project GN05) and the Ministerio de Educación y Ciencia (project CTQ2005-08016). I.V. and G.J.-O. respectively thank the Ministerio de Educación y Ciencia and Universidad de La Rioja for grants.

[1] a) R. J. Deeth, N. Fey, *Organometallics* **2004**, *23*, 1042–1054; b) P. Comba, R. Remenyi, *Coord. Chem. Rev.* **2003**, *238–239*, 9–20; c) D. P. White, W. Douglass in *Computational Organometallic Chemistry* (Ed.: T. R. Cundari), Marcel Dekker, **2001**, 237–274.
[2] a) J. Åqvist, A. Warshel, *Chem. Rev.* **1993**, *93*, 2523–2544; b) F. Jensen, *J. Comput. Chem.* **1994**, *15*, 1199–1216; c) J. E. Eksterowicz, K. N. Houk, *Chem. Rev.* **1993**, *93*, 2439–2461; d) P.-O. Norrby, T. Rasmussen, J. Haller, T. Strassner, K. N. Houk, *J. Am. Chem. Soc.* **1999**, *121*, 10186–10192; e) P.-O. Norrby, *J. Mol. Struct.* **2000**, *506*, 9–16; f) T. Rasmussen, P.-O. Norrby, *J. Am. Chem. Soc.* **2003**, *125*, 5130–5138.
[3] See, for instance: a) A. Mulholland, *Drug Discovery Today* **2006**, *10*, 1393–1402, and references therein; b) R. A. Friesner, V. Guallar, *Ann. Pharm. Belg. Ann. Rev. Phys. Chem.* **2005**, *56*, 389–427; c) S. Martí, M. Roca, J. Andrés, V. Moliner, E. Silla, I. Tuñón, J. Bertrán, *Chem. Soc. Rev.* **2004**, *33*, 98–107; d) M. J. Field, *J. Comput. Chem.* **2002**, *23*, 48–58.
[4] See for instance: a) R. A. Friesner, *Adv. Protein Chem.* **2006**, *72*, 79–104; b) A. Khandelwal, V. Lukacova, D. Comez, D. M. Kroll, S. Raha, S. Balaz, *J. Med. Chem.* **2005**, *48*, 5437–5447; c) A. E. Cho, V. Guallar, B. J. Berne, R. Friesner, *J. Comput. Chem.* **2005**, *26*, 915–931; d) U. Ryde, *Curr. Opin. Chem. Biol.* **2003**, *7*, 136–142.
[5] See for instance: a) A. Magistrato, P. Ruggerone, K. Spiegel, P. Carloni, J. Reedijk, *J. Phys. Chem. B* **2006**, *110*, 3604–3613; b) T. Tuttle, E. Kraka, D. Cremer, *J. Am. Chem. Soc.* **2005**, *127*, 9469–9484; c) K. Spiegel, U. Rothlisberger, P. Carloni, *J. Phys. Chem. B* **2004**, *108*, 2699–2707.
[6] See, for instance: a) O. Acevedo, W. L. Jorgensen, *J. Am. Chem. Soc.* **2006**, *128*, 6141–6146; b) M. Q. Fatmi, T. S. Hofer, B. R. Randolf, B. M. Rode, *Phys. Chem. Chem. Phys.* **2006**, *8*, 1675–1681; c) Y. Mo, J. Gao, *J. Phys. Chem. B* **2006**, *110*, 2976–2980; d) B. M. Rode, C. F. Schwenk, T. S. Hofer, B. R. Randolf, *Coord. Chem. Rev.* **2005**, *249*, 2993–3006; e) I. Fdez, Galván, M. A. Aguilar, M. F. Ruiz-López, *J. Phys. Chem. B* **2005**, *109*, 23024–23030; f) J. Gao, *Acc. Chem. Res.* **1996**, *29*, 298–305; g) J. Gao, *J. Am. Chem. Soc.* **1995**, *117*, 8600–8607.
[7] See, for instance: a) E. A. Ivanova Shor, A. M. Shor, V. A. Naszulov, G. N. Vayssilov, N. Rösch, *J. Chem. Theory Comput.* **2005**, *1*, 459–471; b) J. Fenmann, T. Moniz, O. Kiowski, T. J. McIntire, S. M. Auerbach, T. Vreven, M. J. Frisch, *J. Chem. Theory Comput.* **2005**, *1*, 1232–1239; c) K. Sillar, P. Burk, *J. Phys. Chem. B* **2004**, *108*, 9893–9899.
[8] See for instance: a) A. Genest, A. Woiterski, S. Krüger, A. M. Shor, N. Rösch, *J. Chem. Theory Comput.* **2006**, *2*, 47–58; b) L. Cavallo, A. Correa, C. Costabile, H. Jacobsen, *J. Organomet. Chem.* **2005**, *690*, 5407–5413.
[9] a) T. K. Woo, G. Pioda, U. Röthlisberger, A. Togni, *Organometallics* **2000**, *19*, 2144; b) T. K. Woo, M. Margl, L. Deng, L. Cavallo, T. Ziegler, *Catal. Today* **1999**, *50*, 479.
[10] a) A. M. Segarra, E. Daura-Oller, C. Claver, J. M. Poblet, C. Bo, E. Fernández, *Chem. Eur. J.* **2004**, *10*, 6456–6467; b) E. Daura-Oller, A. M. Segarra, J. M. Poblet, C. Claver, E. Fernández, C. Bo, *J. Org. Chem.* **2004**, *69*, 2669–2680; c) C. Costabile, L. Cavallo, *J. Am. Chem. Soc.* **2004**, *126*, 9592–9600; d) A. Magistrato, T. K. Woo, A. Togni, U. Rothlisberger, *Organometallics* **2004**, *23*, 3218–3227; e) G. Drudis-Solé, G. Ujaque, F. Maseras, A. Lledós, *Chem. Eur. J.* **2005**, *11*, 1017–1029; f) D. Balcells, F. Maseras, G. Ujaque, *J. Am. Chem. Soc.* **2005**, *127*, 3624–3634.
[11] a) F. Maseras, K. Morokuma, *J. Comput. Chem.* **1995**, *16*, 1170; b) F. Maseras, *Top. Organomet. Chem.* **1999**, *4*, 165–191.
[12] M. Svensson, S. Humbel, R. D. J. Froese, T. Matsubara, S. Sieber, K. Morokuma, *J. Phys. Chem.* **1996**, *100*, 19357–19363.
[13] a) A. K. Rappé, C. J. Casewit, K. S. Colwell, W. A. Goddard III, W. M. Skiff, *J. Am. Chem. Soc.* **1992**, *114*, 10024–10035; b) C. J. Casewit, K. S. Colwell, A. K. Rappe, *J. Am. Chem. Soc.* **1992**, *114*, 10035–10046; c) C. J. Casewit, K. S. Colwell, A. K. Rappe, *J. Am. Chem. Soc.* **1992**, *114*, 10046–10053.
[14] a) C. Lee, W. Yang, R. Parr, *Phys. Rev. B* **1988**, *37*, 785–789; b) A. D. Becke, *J. Chem. Phys.* **1993**, *98*, 5648–5652.
[15] S. Niu, M. B. Hall, *Chem. Rev.* **2000**, *100*, 353–406.
[16] a) A. Cornejo, J. M. Fraile, J. I. García, M. J. Gil, V. Martínez-Merino, J. A. Mayoral, L. Salvatella, *Angew. Chem.* **2005**, *117*, 462–465; *Angew. Chem. Int. Ed.* **2005**, *44*, 458–461; b) A. Cornejo, J. M. Fraile, J. I. García, M. J. Gil, V. Martínez-Merino, J. A. Mayoral, L. Salvatella, *Organometallics* **2005**, *24*, 3448–3457.
[17] a) J. M. Fraile, J. I. García, V. Martínez-Merino, J. A. Mayoral, L. Salvatella, *J. Am. Chem. Soc.* **2001**, *123*, 7616–7625; b) J. M. Fraile, J. I. García, M. J. Gil, V. Martínez-Merino, J. A. Mayoral, L. Salvatella, *Chem. Eur. J.* **2004**, *10*, 758–765.
[18] Gaussian 03, Revision C.02, M. J. Frisch, G. W. Trucks, H. B. Schlegel, G. E. Scuseria, M. A. Robb, J. R. Cheeseman, J. A. Montgomery, Jr., T. Vreven, K. N. Kudin, J. C. Burant, J. M. Millam, S. S. Iyengar, J. Tomasi, V. Barone, B. Mennucci, M. Cossi, G. Scalmani, N. Rega, G. A. Petersson, H. Nakatsuji, M. Hada, M. Ehara, K. Toyota, R. Fukuda, J. Hasegawa, M. Ishida, T. Nakajima, Y. Honda, O. Kitao, H. Nakai, M. Klene, X. Li, J. E. Knox, H. P. Hratchian, J. B. Cross, V. Bakken, C. Adamo, J. Jaramillo, R. Gomperts, R. E. Stratmann, O. Yazyev, A. J. Austin, R. Cammi, C. Pomelli, J. W. Ochterski, P. Y. Ayala, K. Morokuma, G. A. Voth, P. Salvador, J. J. Dannenberg, V. G. Zakrzewski, S. Dapprich, A. D. Daniels, M. C. Strain, O. Farkas, D. K. Malick, A. D. Rabuck, K. Raghavachari, J. B. Foresman, J. V. Ortiz, Q. Cui, A. G. Baboul, S. Clifford, J. Cioslowski, B. B. Stefanov, G. Liu, A. Liashenko, P. Piskorz, I. Komaromi, R. L. Martin, D. J. Fox, T. Keith, M. A. Al-Laham, C. Y. Peng, A. Nanayakkara, M. Challacombe, P. M. W. Gill, B. Johnson, W. Chen, M. W. Wong, C. Gonzalez, and J. A. Pople, Gaussian, Inc., Wallingford, CT, **2004**.
[19] C. W. Bauschlicher, Jr., *Chem. Phys. Lett.* **1995**, *246*, 40–44.
[20] J. Le Paih, F. Monnier, S. Dérien, P. H. Dixneuf, E. Clot, O. Eisenstein, *J. Am. Chem. Soc.* **2003**, *125*, 11964–11975.
[21] The partition scheme that considers a butadiene moiety in the QM part of the styrene partition was also tested in the search for the lowest energy TS, for the sake of consistency. As expected, the geometry of the TS found lies between those calculated at the full-QM and QM/MM levels (the latter kept only the ethylene moiety in the QM part of the styrene partition). Additional information can be found in Figure S1 in the Supporting Information.
[22] H. Nishiyama, N. Soeda, T. Naito, Y. Motoyama, *Tetrahedron: Asymmetry* **1998**, *9*, 2865.
[23] a) A. D. Becke, *J. Chem. Phys.* **1997**, *107*, 8554–8560; b) W. Kohn, Y. Meir, D. E. Makarov, *Phys. Rev. Lett.* **1998**, *80*, 4153–4156; c) K. Muller-Dethlefs, P. Hobza, *Chem. Rev.* **2000**, *100*, 143–167; d) T. van Mourik, R. J. Gdanitz, *J. Chem. Phys.* **2002**, *116*, 9620–9623.
[24] T. Rasmussen, J. F. Jensen, N. Èstergaard, D. Tanner, T. Ziegler, P.-O. Norrby, *Chem. Eur. J.* **2002**, *8*, 177–184.
[25] a) B. F. Straub, P. Hofmann, *Angew. Chem.* **2001**, *113*, 1328–1330; *Angew. Chem. Int. Ed.* **2001**, *40*, 1288–1290; b) B. F. Straub, I. Gruber, F. Rominger, P. Hofmann, *J. Organomet. Chem.* **2003**, *684*, 124–143.
[26] K. Suenobu, M. Itagaki, E. Nakamura, *J. Am. Chem. Soc.* **2004**, *126*, 7271–7280.
[27] X. Dai, T. H. Warren, *J. Am. Chem. Soc.* **2003**, *125*, 10085–10094.
[28] a) D. A. Evans, K. A. Woerpel, M. M. Hinman, M. M. Faul, *J. Am. Chem. Soc.* **1991**, *113*, 726–728; b) D. A. Evans, K. A. Woerpel, M. J. Scott, *Angew. Chem. Int. Ed. Engl.* **1992**, *31*, 430–432.
[29] a) J. M. Fraile, J. I. García, C. I. Herrerías, J. A. Mayoral, D. Carrié, M. Vaultier, *Tetrahedron: Asymmetry* **2001**, *12*, 1891–1894.
[30] A. Cornejo, J. M. Fraile, J. I. García, M. J. Gil, V. Martínez-Merino, J. A. Mayoral, E. Pires, I. Villalba, *Synlett* **2005**, 2321–2324.

Received: September 20, 2006
Published online: February 16, 2007

